

Automatic electronic-controlled mode locking self-start in fibre lasers with non-linear polarisation evolution

Daba Radnatarov, Sergey Khripunov,* Sergey Kobtsev, Aleksey Ivanenko, Sergey Kukarin

Division of Laser Physics and Innovative Technologies, Novosibirsk State University, 630090, Novosibirsk, Russia
[*khripunovsa@gmail.com](mailto:khripunovsa@gmail.com)

Abstract: The present work demonstrates a fibre-laser system with automatic electronic-controlled triggering of dissipative soliton generation mode. Passive mode locking based on the effect of non-linear polarisation evolution has been achieved through a polarisation controller containing a single low-voltage liquid crystal plate whose optimal wave delay was determined from analysis of inter-mode beat spectrum of the output radiation.

©2013 Optical Society of America

OCIS codes: (140.4050) Mode-locked lasers; (230.3720) Liquid-crystal devices; (190.4370) Nonlinear optics, fibers.

References and links

1. V. J. Matsas, T. P. Newson, D. J. Richardson, and D. N. Payne, "Self-starting, passively mode-locked fibre ring soliton laser exploiting non-linear polarisation rotation," *Electron. Lett.* **28**(15), 1391–1393 (1992).
2. M. E. Fermann, *Nonlinear polarization evolution in passively mode-locked fiber lasers* (Cambridge University Press, 1995), Chapter 5.
3. B. Oktem, C. Ülgüdür, and Ö. Ilday, "Soliton-similariton fibre laser," *Nat. Photonics* **4**(5), 307–311 (2010), <http://www.nature.com/nphoton/journal/v4/n5/full/nphoton.2010.33.html>.
4. S. V. Smirnov, S. M. Kobtsev, S. V. Kukarin, and S. K. Turitsyn, *Mode-Locked Fibre Lasers with High-Energy Pulses* (InTech, 2011), Chapter 3.
5. W. H. Renninger and F. W. Wise, *Dissipative soliton fiber lasers* (Wiley-VCH Verlag GmbH & Co. KgaA, 2012), Chapter 4.
6. F. Ilday, J. Buckley, L. Kuznetsova, and F. Wise, "Generation of 36-femtosecond pulses from a ytterbium fiber laser," *Opt. Express* **11**(26), 3550–3554 (2003).
7. S. Kobtsev, S. Kukarin, and Y. Fedotov, "Ultra-low repetition rate mode-locked fiber laser with high-energy pulses," *Opt. Express* **16**(26), 21936–21941 (2008).
8. L. M. Zhao, D. Y. Tang, T. H. Cheng, and C. Lu, "Nanosecond square pulse generation in fiber lasers with normal dispersion," *Opt. Commun.* **272**(2), 431–434 (2007), <http://www.sciencedirect.com/science/article/pii/S0030401806012879>.
9. T. Hirooka and M. Nakazawa, "Parabolic pulse generation by use of a dispersion-decreasing fiber with normal group-velocity dispersion," *Opt. Lett.* **29**(5), 498–500 (2004).
10. B. Ortaç, A. Hideur, M. Brunel, C. Chédot, J. Limpert, A. Tünnermann, and F. Ö. Ilday, "Generation of parabolic bound pulses from a Yb-fiber laser," *Opt. Express* **14**(13), 6075–6083 (2006).
11. J. M. Soto-Crespo, P. Grelu, N. Akhmediev, and N. Devine, "Soliton complexes in dissipative systems: vibrating, shaking, and mixed soliton pairs," *Phys. Rev. E Stat. Nonlin. Soft Matter Phys.* **75**(1), 016613 (2007).
12. W. H. Renninger, A. Chong, and F. W. Wise, "Pulse shaping and evolution in normal-dispersion mode-locked fiber lasers," *IEEE J. Sel. Top. Quantum Electron.* **18**(1), 389–398 (2012).
13. S. Smirnov, S. Kobtsev, S. Kukarin, and A. Ivanenko, "Three key regimes of single pulse generation per round trip of all-normal-dispersion fiber lasers mode-locked with nonlinear polarization rotation," *Opt. Express* **20**(24), 27447–27453 (2012).
14. P. Grelu and N. Akhmediev, "Dissipative solitons for mode-locked lasers," *Nat. Photonics* **6**(2), 84–92 (2012), http://www.nature.com/nphoton/journal/v6/n2/abs/nphoton.2011.345.html?WT.mc_id=TWI_NaturePhotonics.
15. N. Imoto, N. Yoshizawa, J. Sakai, and H. Tsuchiya, "Birefringence in single-mode optical fiber due to elliptical core deformation and stress anisotropy," *IEEE J. Quantum Electron.* **16**(11), 1267–1271 (1980).
16. E. Collett, *Polarization Controllers*, (The PolaWave Group, 2003), Chapter 9.
17. A. Chong, J. Buckley, W. Renninger, and F. Wise, "All-normal-dispersion femtosecond fiber laser," *Opt. Express* **14**(21), 10095–10100 (2006).

18. A. Yariv and A. Yariv, *Optical waves in crystals: propagation and control of laser radiation*, Wiley-Interscience, 2002.
19. Z. Zhuang, S. W. Suh, and J. S. Patel, "Polarization controller using nematic liquid crystals," *Opt. Lett.* **24**(10), 694–696 (1999).
20. S. M. Kelly and M. O'Neill, *Liquid crystals for electro-optic applications* (Academic Press, 2000), Chapter 1.
21. A. Safrani and I. Abdulhalim, "Liquid-crystal polarization rotator and a tunable polarizer," *Opt. Lett.* **34**(12), 1801–1803 (2009).
22. L. Wei, T. T. Alkeskjold, and A. Bjarklev, "Tunable and rotatable polarization controller using photonic crystal fiber filled with liquid crystal," *Appl. Phys. Lett.* **96**(24), 241104 (2010), http://apl.aip.org/resource/1/applab/v96/i24/p241104_s1?bypassSSO=1.
23. A. K. Pitolakis, D. C. Zografopoulos, and E. E. Kriezis, "In-line polarization controller based on liquid-crystal photonic crystal fibers," *J. Lightwave Technol.* **29**(17), 2560–2569 (2011).
24. D. A. Radnatarov, S. A. Khripunov, A. V. Ivanenko, and S. M. Kobtsev, "Mode-locked Er fibre laser with variable wave plate based on liquid crystal," in *ICONO/LAT-2013 Conference*, Technical Digest (CD) (Russian Academy of Sciences, Moscow, 2013), paper LWF2.
25. N. N. Akhmediev and A. Ankiewicz, *Dissipative Solitons*, Springer, 2005.
26. A. Chong, W. H. Renninger, and F. W. Wise, "Properties of normal-dispersion femtosecond fiber lasers," *J. Opt. Soc. Am. B* **25**(2), 140–148 (2008).

1. Introduction

Fibre lasers mode-locked due to non-linear polarisation evolution (NPE) [1–5] are unique light sources with broadly controllable pulse duration, energy, and a variety of possible output pulse shapes. They have been reported to produce pulses under 36 fs [6], pulse energies of ~4 μ J (without any additional amplification) [7], as well as rectangular [8] shape, parabolic [9,10] shape, and other pulse shapes and structures [11–13]. Their wide choice of output radiation parameters [14] draws a great deal of attention to these fibre lasers from both the research community and the industry. They suffer, however, from lack of reliable and easily adjustable means of intra-cavity polarisation control. Such controllers based upon mechanical deformation of optical fibre [15,16] (the fibre-coil or rotatable fibre squeezer approach) cannot, as a rule, retain their set parameters for long periods because of plastic deformations in the optical fibre made of amorphous fused silica. Free-space discrete wave plates [17] or electro-optic crystals [18] may also be used as polarisation controllers with the caveat that there must be at least three such elements in order to cover all possible polarisation states: one half-wave phase element and two quarter-wave ones (Q-H-Q waveplate combination [16]). These elements feature long-term stability, although simultaneous automatic control over three polarisation control components poses certain algorithmic challenges. In addition, discrete wave plates must be rotated with relatively slow electro-mechanical drives, and fast electro-optical crystals require high voltages. Therefore, development of a better self-starting mode-locking mechanism in NPE fibre lasers remains an important problem of modern technology.

Application of liquid-crystal based elements (wave plates, photonic fibres, etc.) is a promising approach to the development of an improved electrically-driven polarisation controller [19–24]. This publication presents an implementation of such a possibility and at the same time demonstrates for the first time that a single non-waveguide nematic liquid crystal wave plate driven by a signal of only several volts can be used as a self-starter of passive mode locking in NPE fibre lasers.

2. Experimental set-up

A simplified schematic diagram of the demonstrated laser is given in Fig. 1. The fibre laser's ring cavity contains the following main components: fibre-optical WDM for coupling of pump radiation, 2 m of active Er-doped fibre, 20 m of normal-dispersion (at 1.55 μ m) fibre (NDF), optical isolator, fibre coupler, fibre-based polarisation beam splitter (PBS), and liquid-crystal variable retarder (LC) installed on a U-bench. All these elements are spliced together with

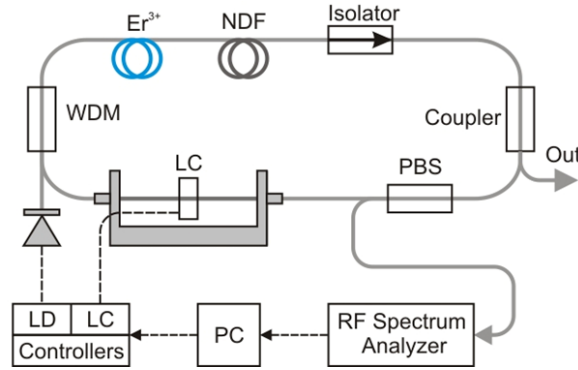


Fig. 1. Experimental layout.

single-mode optical fibre SMF-28, its total length amounting to 5 m. To ensure generation of dissipative solitons with relatively high energies [25, 26], the net positive resonator dispersion was kept at the level of 1 ps^2 owing to a stretch of specialty MetroCore fibre with chromatic dispersion $\beta_2 = 6 \text{ ps}^2$ at $1.55 \mu\text{m}$.

The studied fibre laser was powered with a maximum of 400 mW at 980 nm by coupling the pump radiation into the core of the active single-mode optical fibre through the fibre-optical WDM. The output radiation was branched out of the cavity through a 10% fibre coupler.

The fibre-optical polarisation beam splitter acted as a polarisation-selective element, the radiation from whose output was used for analysis of the laser generation mode. The output radiation was fed into a radio-frequency spectrum analyser by means of a photo-detector.

A single liquid crystal plate was used as variable active phase retarder to control the polarisation state of intra-cavity radiation within certain limits sufficient for starting mode-locked operation. These limits could generally be set by inserting into the cavity additional manually-controlled phase elements, although in our particular case it was possible to avoid any such extra elements by careful manipulation of physical layout of the cavity fibre during the experiment set-up (adjustment of coiling radius, etc.).

In our studies, we could introduce into the resonator a phase delay of 0 to 0.6λ by applying a control voltage not exceeding 4 V to the liquid-crystal plate.

3. Algorithm of programmatically controlled mode lock starting and experimental results

Manual adjustment of pumping radiation power and the voltage applied to the liquid crystal plate did generally induce mode-locked operation, however mode locking starting in this way was not always of sufficient quality. For example, several pulses were observed on the period of cavity round trip time (multi-pulse mode) and mode locking was not stable. In order to determine the optimal control voltage on the liquid crystal cell, we studied its relation to the magnitude of the peak in the radio-frequency inter-mode beat spectrum. This magnitude was measured around the fundamental pulse repetition rate of 8 MHz. The maximum magnitude of this peak corresponded to the most stable mode-locked operation in the absence of any side features in the radio-frequency inter-mode beat spectrum (Fig. 2a). As the magnitude slid off the maximum (due to changing bi-refringence in the liquid crystal cell), the mode lock stability worsened and additional satellite peaks could emerge beside the main one in the radio-frequency beat spectrum (Fig. 2b).

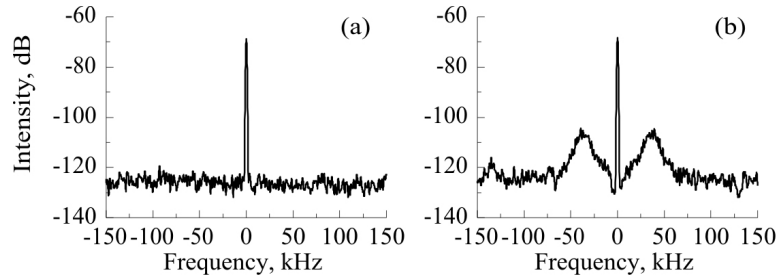


Fig. 2. RF inter-mode beat laser spectrum around 8 MHz typical of the most stable (a) and less stable (b) mode-locked operation.

In this manner, the optimal control voltage on the liquid crystal cell corresponding to the best mode lock stability was established. Further on, we experimentally found out the levels of the laser pump intensity at which single-pulse mode locking was observed. On the basis of these results, an automatic algorithm of single-pulse mode lock triggering was proposed and successfully implemented. The temporal diagram of this algorithm is shown in the following Fig. 3.

The starting phase (I) of the algorithm corresponds to ramping up the pump output power until the mode-locked operation is triggered. For the laser in question, the threshold level of pump radiation P_{thr} , at which mode-locked operation was initiated regardless of the delay introduced by the liquid crystal element, was found to equal 250 mW. When this critical value was exceeded, an unstable multi-pulse mode-locked regime was generally started. After that, during phase II of the algorithm, the voltage applied to the liquid crystal cell was in turn ramped up to the optimal value V_{opt} . Figure 3 demonstrates the full swing of voltages applied to the liquid crystal cell to illustrate the dependence of the magnitude of the peak of the radio-frequency inter-mode beat spectrum on this voltage (dashed line). However, in a practical implementation of the algorithm, the ramp-up of voltage V_{LC} can be stopped at V_{opt} . During the subsequent phase (III) of the algorithm, the pump radiation power was gradually reduced until the multi-pulse mode-locking operation transitioned to the single-pulse one. In the studied laser, this corresponded to the pump radiation power of 50 mW, the mean output power of the laser amounting to 2.5 mW.

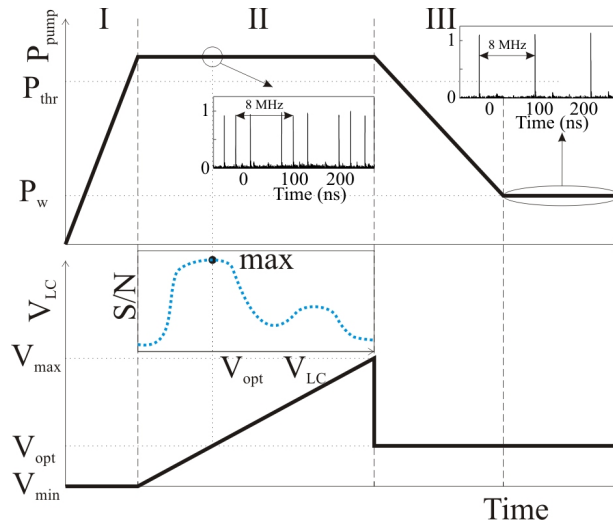


Fig. 3. Time diagram of the programmatically controlled laser mode lock starting: P – pump radiation power; V – control voltage on the liquid crystal plate; dashed line – dependence of the magnitude of the peak of the radio-frequency inter-mode beat spectrum on the voltage applied to the liquid crystal cell.

Reduction of the pumping radiation power in phase III of the algorithm was also accompanied by a transformation of the laser's output radiation spectrum. At pumping power $P > P_{\text{thr}}$, the output spectrum featured a central peak corresponding to laser's CW radiation and incomplete mode locking (Fig. 4, left). In Fig. 4 (right), we show the output spectrum of the laser at reduced pumping power that corresponds to complete mode locking and a stable single-pulse operation.

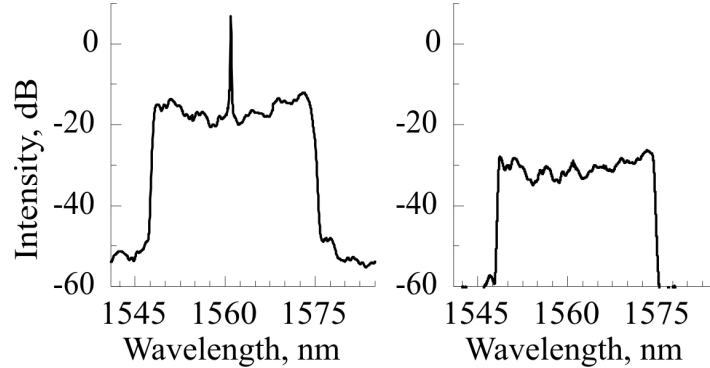


Fig. 4. Left – Optical spectrum of the output radiation at the pump power equal to P_{thr} ; right – output radiation spectrum at the pump power equal to P_w .

In order to measure the pulse duration, the laser's output power was boosted to 100 mW with an external amplifier made of 4-m long DC Er/Yb fibre. Since the amplifier had anomalous net dispersion, the generated pulses were additionally compressed in the process. Auto-scanning correlator FS-PS-Auto from Tekhnoscan was used in these measurements. The recorded auto-correlation function is presented in Fig. 5 and corresponds to pulses with approximately 170-fs duration. The amplified pulses are close to being spectrally limited, taking into account the radiation spectrum width of 23 nm (Fig. 4, right).

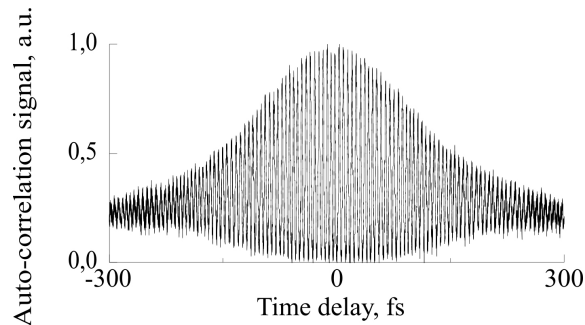


Fig. 5. The recorded auto-correlation function of the laser's output.

4. Conclusions

The present work has for the first time demonstrated an Er-fibre laser with automatic programmatically controlled starting of passively mode-locked operation based on the effect of non-linear polarisation evolution of radiation. A single liquid-crystal wave plate with phase delay controllable through application of low voltage (few V) was used to trigger mode-locked operation. The proposed and successfully tested algorithm for automatic triggering of stable single-pulse mode locking opens new prospects of practical application of fibre lasers, in which mode locking is achieved through non-linear polarisation evolution of radiation.

The created laser ensured reliable triggering of stable mode-locked regime even in the presence of mechanical perturbations leading to its collapse. It has also proven insensitive to local changes in the laser cavity temperature within the range of 20 °C to 100 °C. Therefore,

the proposed algorithm of automatic starting of stable single-pulse mode-locked operation in fibre lasers not relying upon saturable absorbers (which suffer from limited life time) will enable development of reliable ultrafast fibre lasers insensitive to external perturbations.

Acknowledgments

This work was supported by the Marie-Curie International Exchange Scheme, Research Executive Agency Grant “TelaSens” No 269271; Grants of Ministry of Education and Science of the Russian Federation (agreement No. 14.B25.31.0003; project No. 01200907579; agreement No. 14.B37.21.0452, project No. ZN-004); Council of the President of the Russian Federation for the Leading Research Groups of Russia (project No. NSH-2979.2012.2).